



Thermal Hall conductivity as a probe of gap structure in multiband superconductors: The case of $\text{Ba}_{1-x}\text{K}_x\text{Fe}_2\text{As}_2$

J. G. Checkelsky,^{1,*} R. Thomale,² Lu Li,^{1,†} G. F. Chen,³ J. L. Luo,³ N. L. Wang,³ and N. P. Ong¹

¹*Department of Physics, Princeton University, Princeton, New Jersey 08544, USA*

²*Department of Physics, Stanford University, Stanford, California 94305, USA*

³*Beijing National Laboratory, Institute of Physics, Chinese Academy of Sciences, Beijing 100080, China*

(Received 22 January 2012; revised manuscript received 10 October 2012; published 6 November 2012)

The sign and profile of the thermal Hall conductivity κ_{xy} gives important insights into the gap structure of multiband superconductors. With this perspective, we have investigated κ_{xy} and the thermal conductivity κ_{xx} in $\text{Ba}_{1-x}\text{K}_x\text{Fe}_2\text{As}_2$ which display large peak anomalies in the superconducting state. The anomalies imply that a large holelike quasiparticle (QP) population exists below the critical temperature T_c . We show that the QP mean free path inferred from κ_{xx} reproduces the observed anomaly in κ_{xy} , providing a consistent estimate of a large QP population. Further, we demonstrate that the peak structure and holelike signal are consistent with a theoretical scenario where, despite potentially large gap variations on the electron pockets, the minimal homogeneous gap of the superconducting phase resides at a hole pocket. Implications for probing the gap structure in the broader class of pnictide superconductors are discussed.

DOI: [10.1103/PhysRevB.86.180502](https://doi.org/10.1103/PhysRevB.86.180502)

PACS number(s): 74.25.F-, 74.25.Jb, 74.70.Xa

The discovery¹⁻⁵ of superconductivity in the iron pnictides has galvanized intense interest in this new class of superconductors. As in the cuprates, one of the key issues has been the determination of the gap symmetry.⁶ While for a large class of pnictides theory has quickly converged on an s_{\pm} order parameter which changes sign between hole and electron pockets,⁷⁻¹¹ many questions remain regarding the actual form of superconducting pairing, such as gap anisotropies, awaiting further experimental investigation.¹² Among the evidence from measurements on $\text{Ba}_{1-x}\text{K}_x\text{Fe}_2\text{As}_2$, nuclear magnetic resonance (NMR) relaxation experiments¹³⁻¹⁶ appear to be consistent with a multigap scenario of singlet pairing, and penetration depth¹⁷ as well as thermal conductivity¹⁸ experiments suggest the presence of strong gap variations inducing close-to-nodal behavior. Alternatively, angle-resolved photoemission spectroscopy (ARPES) experiments¹⁹⁻²¹ favor an isotropic multiple gap scenario, with higher confidence for the hole pockets located at Γ than for the electron pockets at M .

If the gap parameter $\Delta(\mathbf{k})$ is isotropic on each Fermi surface (FS) sheet, the population of Bogoliubov quasiparticles decreases sharply below T_c (\mathbf{k} is a wave vector on the FS). By contrast, if nodes exist in $\Delta(\mathbf{k})$ (or if $|\Delta(\mathbf{k})|$ is strongly anisotropic), the quasiparticle (QP) population decreases quite gradually. In effective single-band superconductors with unconventional gap symmetry, the thermal Hall conductivity κ_{xy} has proved to be a powerful probe for quasiparticles (QPs). Unlike the diagonal thermal conductivity κ_{xx} , which is the sum of the electronic term κ_e and the phonon term κ_{ph} , the off-diagonal term κ_{xy} is purely electronic. Together, κ_{xx} and κ_{xy} have been used to probe extensively the QP density and their lifetime in the cuprate $\text{YBa}_2\text{Cu}_3\text{O}_y$ (YBCO)²²⁻²⁴ and the heavy fermion superconductor CeCoIn_5 .^{25,26} In contrast to effective single-band descriptions of the above compounds, the pnictides are manifestly multiband superconductors with both electronlike and holelike Fermi pockets. We report thermal Hall results which connect to the following insight: Whether the thermal Hall signal is electronlike or holelike yields

nontrivial information in the presence of potentially both holelike and electronlike low-lying charge carriers. In principle, this also applies to thermopower experiments,²⁷ though such electrical probes are restricted to the nonsuperconducting state. For the pnictides, this provides valuable consistency checks of different theoretical gap scenarios, as we explicate in the following for the specific case of $\text{Ba}_{1-x}\text{K}_x\text{Fe}_2\text{As}_2$. There, we find theoretically that while the largest gap anisotropy exists along the electron pockets, the lowest gap resides at a hole pocket, which is consistent with our findings from thermal Hall conductivity.

To begin, we report detailed measurements of $\kappa_{xx}(T, H)$ and $\kappa_{xy}(T, H)$ on single crystals of $\text{Ba}_{1-x}\text{K}_x\text{Fe}_2\text{As}_2$ in the geometry with the field $\mathbf{H} \parallel \hat{z} \parallel \hat{c}$ and $-\nabla T \parallel \hat{x}$. The longitudinal and transverse temperature gradients δT_x and δT_y were measured using chromel-alumel thermocouples. The two crystals studied have dimensions $2 \times 1 \times 0.1 \text{ mm}^3$. At 10 K, the resolution achieved is $\delta T_y \sim 10 \text{ mK}$. Measurements of κ_{xy} were made to a field up to 14 T using thermocouples. To extend measurements of κ_{xx} below 6 K where the thermocouple sensitivity falls steeply, we used matched RuO_x microsensors which are very sensitive below 4 K (measurements were performed to $H = 35 \text{ T}$). Electrical measurements are performed using standard four-probe techniques using a lock-in amplifier. All measurements are performed in a vacuum atmosphere.

Figure 1(a) plots the T dependence of $\kappa_{xx}(T, H)$ in sample 1 with $H = 0$ (circles) and with $H = 35 \text{ T}$ (triangles), together with the in-plane resistivity ρ (solid curve). The curve for $\kappa_{xx}(T, 0)$ is closely similar in sample 2. As shown, $\kappa_{xx}(T, 0)$ is nearly T independent between T_c ($=37 \text{ K}$) and 100 K. Below T_c , it rises to a broad maximum that peaks near $\frac{1}{2}T_c$. In a 35-T field, the anomaly is almost completely suppressed. In the Boltzmann theory approach, κ_e from QP excitations is given by^{28,29}

$$\kappa_e = \frac{4}{T} \sum_{\mathbf{k}} \left(-\frac{\partial f_0}{\partial E_{\mathbf{k}}} \right) E_{\mathbf{k}}^2 v_x^2(\mathbf{k}) \tau(\mathbf{k}), \quad (1)$$

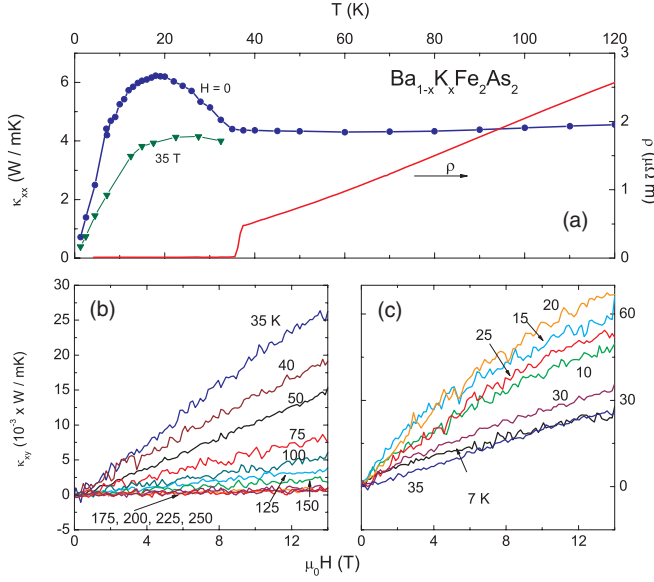


FIG. 1. (Color online) (a) κ_{xx} of single-crystal $\text{Ba}_{1-x}\text{K}_x\text{Fe}_2\text{As}_2$ at $H = 0$ (circles) and at 35 T (triangles). The solid curve is the in-plane resistivity ρ in zero H ($T_c = 37$ K). κ_{xy} vs H at $T = 250 \rightarrow 35$ K and from 35 \rightarrow 7 K are shown in (b) and (c), respectively. Above T_c (37 K), κ_{xy} is H linear up to 14 T, but as T decreases below T_c , the curvature becomes increasingly apparent. At all T , the Hall signal is holelike.

where $E_{\mathbf{k}} = \sqrt{\Delta(\mathbf{k})^2 + \epsilon_{\mathbf{k}}^2}$ is the QP energy with $\epsilon_{\mathbf{k}}$ the normal-state energy. Here, $\mathbf{v}(\mathbf{k})$ is the QP group velocity, f_0 the Fermi-Dirac distribution, and $\tau(\mathbf{k})$ the transport relaxation time. A recent treatment of κ_{xy} applied to YBCO is given by Durst *et al.*³⁰ Both the anomaly profile and its field suppression are similar to features seen in YBCO and CeCoIn₅. In these unconventional superconductors, κ_{xx} also rises to a large peak near $\frac{1}{2}T_c$, reflecting a large QP population and a greatly enhanced (zero-field) QP mean free path ℓ_0 . By contrast, κ_{xx} decreases roughly linearly with $(T_c - T)$ below T_c in the clean s -wave superconductors Pb, Hg, and Sn (Refs. 28 and 29) (data on κ_{xy} are unavailable).

The curves of κ_{xy} vs H at fixed T are displayed in Figs. 1(b) and 1(c). Both above and below T_c , the sign of κ_{xy} is positive (holelike). Above T_c , κ_{xy} is strictly linear in H (up to 14 T). As T decreases from 100 K to T_c , the slope of κ_{xy} vs H increases gradually until T_c , where it undergoes a sharp increase. In the normal state, κ_{xy} originates from the Lorentz force acting on the charge carriers (the Hall effect is also holelike). Below T_c , the scattering of QPs from pinned vortex lines possesses a right-left asymmetry which leads to a large κ_{xy} .^{22,30,31} The asymmetry originates from the circulation of the supercurrent around the vortex core and the Volovik effect.³² The QP Hall current initially scales linearly with the vortex line density $n_V = |B|/\phi_0$, where B is the flux density and ϕ_0 is the superconducting flux quantum. At large B , however, vortex scattering also reduces the mean free path of the QPs (see below), resulting in a negative curvature in $\kappa_{xy}(H)$. In Fig. 1(c), the steady increase in curvature is seen as T decreases from 20 to 7 K.

Focusing on the weak- H regime, we see that the sharp change at T_c in the QP Hall conductivity κ_{xy} is apparent when

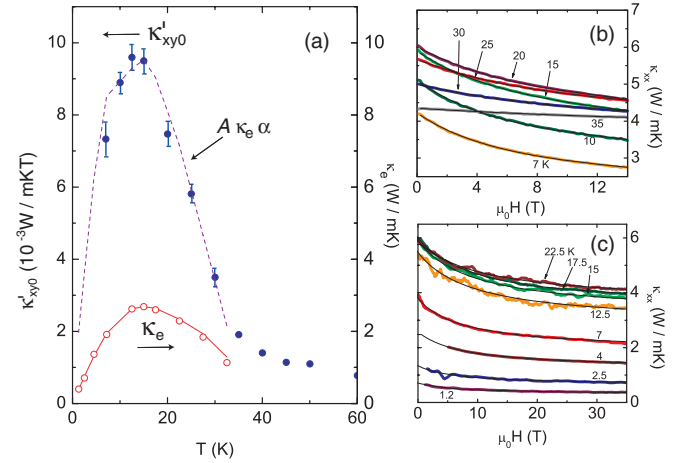


FIG. 2. (Color online) (a) T dependence of the weak-field slope $\kappa'_{xy0} \equiv \lim_{H \rightarrow 0} \kappa_{xy}/H$ (solid circles with error bars). As T falls below T_c , κ'_{xy0} displays a steep increase to reach a peak at 18 K. For comparison, the quantity $A\alpha\kappa_e$ (with $A = 0.033$, see below) is plotted as the dashed curve, and the electronic term κ_e , inferred from Eq. (2), is displayed as open circles. Curves of κ_{xx} vs H at fixed T measured with thermocouples to 14 T (b) and with RuO_x sensors to 35 T (c). In both, fits to Eq. (2) are shown as thin curves.

we plot the weak-field slope $\kappa'_{xy0} \equiv \lim_{H \rightarrow 0} \kappa_{xy}/H$ [solid circles in Fig. 2(a)]. As T decreases from 200 K to T_c , κ'_{xy} increases slowly by a factor of ~ 3 . At T_c , κ'_{xy0} exhibits a sharp break in slope, followed by a steeper rise to a peak that is ~ 5 times larger than its value at T_c (curves of $A\kappa_e\alpha$ and κ_e are discussed below).

We next turn to the diagonal term $\kappa_{xx}(T, H)$, which provides quantitative estimates of the electronic term κ_e and ℓ_0 independent of κ_{xy} [Figs. 2(b) and 2(c)]. In the normal state, over the interval 250–40 K, the field dependence of κ_{xx} is undetectable with our sensitivity. Just below T_c , a weak H dependence becomes apparent (curve at 35 K). As T decreases, this rapidly evolves to a singular $|B|$ dependence that characterizes the scattering of QPs from pinned vortices in type-II superconductors in the clean limit ($\ell_0 \gg \xi$, where ξ is the coherence length).

The data in Figs. 2(b) and 2(c) fit well to the vortex-scattering expression (shown as thin curves)^{22,30,31}

$$\kappa_{xx}(T, B) = \frac{\kappa_e(T)}{1 + \alpha(T)|B|} + \kappa_{\text{ph}}(T), \quad (2)$$

where $\alpha(T) = \ell_0\sigma_{\text{tr}}/\phi_0$ with σ_{tr} the vortex cross section presented to an incident QP. Equation (2) expresses the additivity of the zero- H scattering rate ($\sim \ell_0^{-1}$) and the scattering rate introduced by vortices $\ell_v^{-1} = \sigma_{\text{tr}}n_V$. Because $H_{c2} > 80$ T,³³ the condensate amplitude is nearly unaffected by the applied H . Hence we can assume that $\kappa_e(T)$ is nearly independent of H , and the dominant contribution to the observed H dependence arises from vortex scattering. We have assumed that the phonon term κ_{ph} has negligible H dependence, consistent with $q\xi \ll 1$, where q is the average phonon wave vector for $T < T_c$.

From the fits to the curves in Fig. 2, we have determined $\kappa_e(T)$, $\kappa_{\text{ph}}(T)$, and $\alpha(T)$. As shown in Fig. 3(a), the phonon term κ_{ph} decreases monotonically as T decreases below T_c .

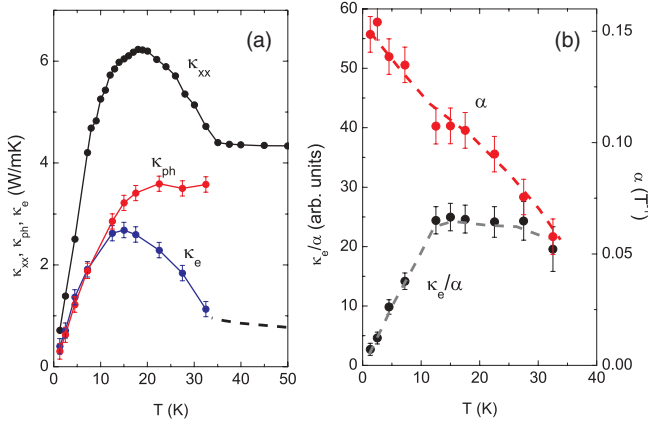


FIG. 3. (Color online) (a) Comparison of κ_{xx} with κ_e and κ_{ph} inferred from fits of curves in Figs. 2(b) and 2(c) to Eq. (2). Above T_c , κ_e is less than $\frac{1}{3}\kappa_{xx}$. Below T_c , however, κ_e increases rapidly to account for the observed anomaly in the observed κ_{xx} . (b) displays $\alpha = \ell_0\sigma_{tr}/\phi_0$ and κ_e/α obtained from the fits. With $\sigma_{tr} \sim 26 \text{ \AA}$, we estimate that $\ell_0 \simeq 1200 \text{ \AA}$ at 2 K. The quantity κ_e/α is a measure of the QP population below T_c .

By contrast, the zero- H electronic term κ_e rises to a broad maximum at 15 K and then falls. As evident, the monotonic profile of κ_{ph} implies that the peak in κ_{xx} (in zero H) is entirely associated with κ_e . In turn, the large peak in κ_e demands a large QP population that survives to $\sim \frac{1}{2}T_c$. The profile of $\kappa_e(T)$ is similar to the anomalously enhanced QP conductivity $\sigma_1(T)$ reported in penetration depth experiments,¹⁷ consistent with a common QP origin.

The fits also yield estimates of $\alpha = \ell_0\sigma_{tr}/\phi_0$ which we display in Fig. 3(b). As T decreases from 35 to 1.2 K, α rises to $3\times$ the value at T_c . This reflects primarily the increase in ℓ_0 . According to Cleary,³¹ the cross section $\sigma_{tr} \simeq \xi$. With the estimate $\xi \simeq 20 \text{ \AA}$ (from $H_{c2} \sim 85 \text{ T}$), we find that α at 1.2 K corresponds to $\ell_0 \simeq 1200 \text{ \AA}$. This supports our assumption that $\text{Ba}_{1-x}\text{K}_x\text{Fe}_2\text{As}_2$ is in the clean limit $\ell_0 \gg \xi$, as has been widely reported. We also note that the onset of curvature in $\kappa_{xy}(B)$ is consistent with this estimate as it reflects the curtailing of ℓ_0 by the vortex-scattering mean free path $\ell_v = \phi_0/\sigma_{tr}|B|$. Since κ_e is proportional to ℓ_0 , a nominal picture of the T dependence of the QP population may be obtained from the ratio κ_e/α . This quantity is plotted as in Fig. 3(b). Initially, κ_e/α is nominally T independent, but decreases linearly with T below 13 K. While similar profiles have been reported previously in nodal superconductors,²² here this phenomenon is rooted in the multiband nature of superconductivity, which deserves further study.

The fits of κ_{xx} vs H to Eq. (2) has allowed us to determine κ_e , κ_{ph} , and α independent of κ_{xy} . To show that these estimates are consistent with the thermal Hall conductivity, we note that $\kappa'_{xy0} \sim \ell_0^2$ should share the same T dependence as $\alpha\kappa_e \sim \ell_0^2$, in the semiclassical approximation. In Fig. 2(a), we have plotted $A\kappa_e\alpha$ with the scale factor $A = 0.033$ (dashed curve) to compare it with the measured values of κ'_{xy0} . Within the uncertainty inherent in κ'_{xy0} , the T dependences may be seen to track each other quite well, especially between 12 and 35 K. Hence, both κ_{xx} and κ_{xy} indicate a large holelike QP population that persists down to $T \sim \frac{1}{2}T_c$. Moreover, the values of $\alpha \sim$

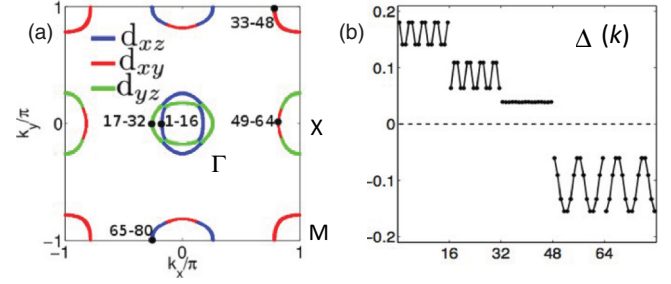


FIG. 4. (Color online) Band structure (a) and SC gap function (b) for the 122 band structure around optimally hole-doped filling. The different dominant d orbital weights are plotted along the Fermi surface in (a) indicated by blue, green, and red. The pockets are divided into 80 momentum patches enumerated counterclockwise (a).

ℓ_0 inferred from κ_{xx} give a consistent description of the T dependences of both κ_e and κ'_{xy0} .

The experimental evidence of large low-lying holelike QP weight we obtain from our thermal Hall measurement can be reconciled with a theoretical perspective on the problem. Starting from a simplified band structure fit for $\text{Ba}_{1-x}\text{K}_x\text{Fe}_2\text{As}_2$,³⁴ the Fermi surface topology is schematically depicted in Fig. 4(a) in the unfolded Brillouin zone with one Fe atom per unit cell. As seen there, the d_{xz} and d_{yz} Fe orbitals dominate the hole pockets at Γ , while the third hole pocket at M is composed of d_{xy} . (The third hole pocket at M which also maps onto the Γ point in the folded Brillouin zone has been detected in ARPES being of nearly identical size and shape as one of the other hole pockets.^{21,35}) The electron pockets at $X = (\pi,0)/(0,\pi)$ involve weights of all three of these d orbitals. Assuming that inter-pocket scattering is dominated by intraorbital interactions, various theoretical approaches predict a significant gap anisotropy on the electron pockets as a consequence of frustrated electron-electron and electron-hole scattering,^{36,37} while the hole pocket gaps are assumed to be rather homogeneous. In a four-pocket scenario where the hole pocket at M is absent, it would hence be a natural guess that the weakest gap can be found on the electron pockets,³⁶ and as a consequence that the thermal Hall signal in the superconducting (SC) phase should be electronlike. In contrast, the hole pocket at M significantly changes the situation: Figure 4(b) shows the gap function $\Delta(k)$ which we have computed by the multiorbital functional renormalization group,^{36,38-40} with interaction parameters as chosen in Ref. 41. To begin with, we find the sign change from hole to electron pockets, as is characteristic for an s_{\pm} order parameter. The largest gap anisotropy is found on the electron pockets. However, we find the smallest amplitude to be located on the hole pocket at M . This is because most of the scattering of this pocket is governed by the subdominant interorbital repulsion scale, as only a small part of the electron pockets share the d_{xy} orbital content. In addition, the available phase space for QPs is quite large on the pocket (or at least comparable to the other pockets), which is consistent with the dominant holelike QP profile of the thermal Hall conductivity measurements.

Let us connect our analytical finding in Fig. 4 with our κ_{xx} measurement in Fig. 3. There, we see a persistent QP weight below T_c . This would be very unusual for a single-pocket

superconductor: Transcending from the normal to the superconducting state, the pairing should in principle reduce the available QP weight below T_c . This is different in the multiband (multipocket) case; κ_e as in Eq. (1) has contributions from each band. Since the hole QPs from the M band exhibit the weakest pairing, κ_{xx} rises abruptly below T_c , signaling enhanced QP character (Fig. 3). With the corresponding Δ remaining relatively small even appreciably below T_c , this may act to mimic the behavior of a nearly nodal single gap compound. In addition to the reported suppression of the QP scattering rate, we hypothesize that the anomalous behavior in $\sigma_1(T)$ reported in penetration depth experiments has a similar multiband origin.¹⁷ Similarly, measurements of the nuclear-spin-lattice relaxation rate in this compound have shown a lack of both a Hebel-Slichter peak and exponential T dependence below T_c , recently attributed to the multiband character of superconductivity.^{12,16}

We propose extending thermal Hall measurements beyond optimally doped $\text{Ba}_{1-x}\text{K}_x\text{Fe}_2\text{As}_2$ will provide an incisive test to gain experimental insight into the nature of multiband superconducting pairing mechanisms in general. For example, for further K doping we expect the holelike profile to persist and become even more pronounced, as d -wave order can form and even give rise to nodes on the hole pockets.³⁶ Moving to the electron-doped side through Co doping should eventually remove the broad hole band, giving rise to the hole

pocket at M from the Fermi surface, by which the small gap regimes on the electron pockets should become the dominant contribution to low-energy charge carriers. We hence predict a sign change of the thermal Hall signal as a function of doping. Similar trends may be triggered by a stronger nodal propensity due to isovalent doping of the As-based compound by P, potentially giving rise to accidental nodes on the electron pockets.^{36,42} It may likewise be interesting to investigate the recently discovered iron chalcogenides such as $\text{K}_x\text{Fe}_2\text{Se}_2$,^{43,44} where the potential role of holelike carriers may be intimately linked to the competition between a possible s_{\pm} and gapped d -wave order parameter.^{45–47} As a result, it is likely that the properties of the quasiparticles extracted from heat transport will be valuable for understanding the pairing mechanism of multiband superconductors.

We thank P. A. Lee, D.-H. Lee, S. Graser, D. Scalapino, B. A. Bernevig, and M. Z. Hasan for helpful discussions. The research at Princeton is supported by US National Science Foundation (NSF) under Grant No. DMR-0819860. Research at IOP is supported by NSFC, 973 project of MOST, and CAS of China. High-field experiments were performed at the National High Magnetic Field Laboratory, Tallahassee, a national facility supported by NSF, the Department of Energy, and the State of Florida. R.T. is supported by an SITP fellowship by Stanford University and DFG-SPP 1458.

*Present address: Department of Applied Physics, University of Tokyo, Tokyo, Japan.

[†]Present address: Department of Physics, University of Michigan, Ann Arbor, MI 48109.

¹Y. Kamihara, T. Watanabe, M. Hirano, and H. Hosono, *J. Am. Chem. Soc.* **130**, 3296 (2008).

²Z. Ren *et al.*, *Chin. Phys. Lett.* **25**, 2215 (2008).

³G. F. Chen, Z. Li, D. Wu, G. Li, W. Z. Hu, J. Dong, P. Zheng, J. L. Luo, and N. L. Wang, *Phys. Rev. Lett.* **100**, 247002 (2008).

⁴X. H. Chen, T. Wu, G. Wu, R. H. Liu, H. Chen, and D. F. Fang, *Nature (London)* **453**, 761 (2008).

⁵C. de la Cruz *et al.*, *Nature (London)* **453**, 899 (2008).

⁶D. N. Basov and A. V. Chubukov, *Nat. Phys.* **7**, 272 (2011).

⁷I. I. Mazin, D. J. Singh, M. D. Johannes, and M. H. Du, *Phys. Rev. Lett.* **101**, 057003 (2008).

⁸K. Kuroki, S. Onari, R. Arita, H. Usui, Y. Tanaka, H. Kontani, and H. Aoki, *Phys. Rev. Lett.* **101**, 087004 (2008).

⁹V. Stanev, J. Kang, and Z. Tesanovic, *Phys. Rev. B* **78**, 184509 (2008).

¹⁰A. V. Chubukov, D. V. Efremov, and I. Eremin, *Phys. Rev. B* **78**, 134512 (2008).

¹¹S. Graser, T. A. Maier, P. J. Hirschfeld, and D. J. Scalapino, *New J. Phys.* **11**, 025016 (2009).

¹²P. J. Hirschfeld, M. M. Korshunov, and I. I. Mazin, *Rep. Prog. Phys.* **74**, 124508 (2011).

¹³Y. Nakai, K. Ishida, Y. Kamihara, M. Hirano, and H. Hosono, *J. Phys. Soc. Jpn.* **77**, 073701 (2008).

¹⁴K. Matano *et al.*, *Eur. Phys. Lett.* **87**, 27012 (2009).

¹⁵H. Fukazawa *et al.*, *J. Phys. Soc. Jpn.* **78**, 033704 (2009).

¹⁶M. Yashima *et al.*, *J. Phys. Soc. Jpn.* **78**, 103702 (2009).

¹⁷K. Hashimoto *et al.*, *Phys. Rev. Lett.* **102**, 207001 (2009).

¹⁸X. G. Luo *et al.*, *Phys. Rev. B* **80**, 140503 (2009).

¹⁹H. Ding *et al.*, *Eur. Phys. Lett.* **83**, 47001 (2008).

²⁰L. Wray *et al.*, *Phys. Rev. B* **78**, 184508 (2008).

²¹H. Ding *et al.*, *J. Phys.: Condens. Matter* **23**, 135701 (2011).

²²K. Krishana, J. M. Harris, and N. P. Ong, *Phys. Rev. Lett.* **75**, 3529 (1995).

²³B. Zeini, A. Freimuth, B. Buchner, R. Gross, A. P. Kampf, M. Klaser, and G. Muller-Vogt, *Phys. Rev. Lett.* **82**, 2175 (1999).

²⁴Y. Zhang, N. P. Ong, P. W. Anderson, D. A. Bonn, R. Liang, and W. N. Hardy, *Phys. Rev. Lett.* **86**, 890 (2001).

²⁵K. Izawa, H. Yamaguchi, Y. Matsuda, H. Shishido, R. Settai, and Y. Onuki, *Phys. Rev. Lett.* **87**, 057002 (2001).

²⁶Y. Onose, N. P. Ong, and C. Petrovic, *Europhys. Lett.* **80**, 37005 (2007).

²⁷Y. J. Yan, X. F. Wang, R. H. Liu, H. Chen, Y. L. Xie, J. J. Ying, and X. H. Chen, *Phys. Rev. B* **81**, 235107 (2010).

²⁸J. Bardeen, G. Rickayzen, and L. Tewordt, *Phys. Rev.* **113**, 982 (1959).

²⁹L. Tewordt, *Phys. Rev.* **129**, 657 (1963).

³⁰A. C. Durst, A. Vishwanath, and P. A. Lee, *Phys. Rev. Lett.* **90**, 187002 (2003).

³¹R. M. Cleary, *Phys. Rev.* **175**, 587 (1968).

³²G. Volovik, *JETP Lett.* **58**, 469 (1993).

³³N. Ni, S. L. Budko, A. Kreyssig, S. Nandi, G. E. Rustan, A. I. Goldman, S. Gupta, J. D. Corbett, A. Kracher, and P. C. Canfield, *Phys. Rev. B* **78**, 014507 (2008).

³⁴S. Graser, A. F. Kemper, T. A. Maier, H.-P. Cheng, P. J. Hirschfeld, and D. J. Scalapino, *Phys. Rev. B* **81**, 214503 (2010).

- ³⁵L. A. Wray, R. Thomale, C. Platt, D. Hsieh, D. Qian, G. F. Chen, J. L. Luo, N. L. Wang, and M. Z. Hasan, *Phys. Rev. B* **86**, 144515 (2012).
- ³⁶R. Thomale, C. Platt, W. Hanke, and B. A. Bernevig, *Phys. Rev. Lett.* **106**, 187003 (2011).
- ³⁷W. Hanke, C. Platt, and R. Thomale, *Ann. Phys. (Berlin)* **523**, 638 (2011).
- ³⁸F. Wang, H. Zhai, Y. Ran, A. Vishwanath, and D.-H. Lee, *Phys. Rev. Lett.* **102**, 047005 (2009).
- ³⁹R. Thomale, C. Platt, J. Hu, C. Honerkamp, and B. A. Bernevig, *Phys. Rev. B* **80**, 180505 (2009).
- ⁴⁰C. Platt, C. Honerkamp, and W. Hanke, *New J. Phys.* **11**, 055058 (2009).
- ⁴¹R. Thomale, C. Platt, W. Hanke, J. Hu, and B. A. Bernevig, *Phys. Rev. Lett.* **107**, 117001 (2011).
- ⁴²K. Kuroki, H. Usui, S. Onari, R. Arita, and H. Aoki, *Phys. Rev. B* **79**, 224511 (2009).
- ⁴³J. Guo, S. Jin, G. Wang, S. Wang, K. Zhu, T. Zhou, M. He, and X. Chen, *Phys. Rev. B* **82**, 180520 (2010).
- ⁴⁴M. H. Fang *et al.*, *Eur. Phys. Lett.* **94**, 27009 (2011).
- ⁴⁵F. Wang, F. Yang, M. Gao, Z.-Y. Lu, T. Xiang, and D. H. Lee, *Eur. Phys. Lett.* **93**, 57003 (2011).
- ⁴⁶T. A. Maier, S. Graser, P. J. Hirschfeld, and D. J. Scalapino, *Phys. Rev. B* **83**, 100515 (2011).
- ⁴⁷C. Fang, Y.-L. Wu, R. Thomale, B. A. Bernevig, and J. Hu, *Phys. Rev. X* **1**, 011009 (2011).